THE EFFECT OF IMPINGEMENT HOT AIR ON TEMPERATURE DISTRIBUTION OF THE FLAT PLATE

By:

NOR ASIKIN BINTI ABU KASIM

(Matrix no.: 140070)

Supervisor:

Dr. Mohd Azmi Bin Ismail

July 2021

This dissertation is submitted to
Universiti Sains Malaysia
As partial fulfillment of the requirement to graduate with honours degree in
BACHELOR OF ENGINEERING (MECHANICAL ENGINEERING)

School of Mechanical Engineering
Engineering Campus
Universiti Sains Malaysia

DECLARATION

I hereby declare that the project report titled "The Effect of Impingement Hot Air on the Temperature Distribution of the Flat Plate" that I submitted to the School of Mechanical Engineering, Engineering Campus, Universiti Sains Malaysia in partial fulfilment of the requirement for the award of the degree of Bachelor of Engineering (Mechanical Engineering) is an authentic record of the projects I worked. To the best of my knowledge, the facts and data included in this report are genuine, and I wrote and performed it. Additionally, I declare that the work detailed in this project has not been submitted and will not be submitted for the award of any other degree, diploma, or fellowship at this institution or any other university or institute, in whole or in part. Additionally, I declare my competence with the terms' plagiarism' and 'copyright'. I am entirely liable for any repercussions resulting from a breach of these rules (if any are discovered in the study project report). Turnitin software was used to evaluate the project report for plagiarism. With my permission as University Supervisor, I have submitted this research project report for evaluation.

30.07.2021

(Date)

Nor Asikin Binti Abu Kasim

30.07.2021

(Date)

Dr. Mohd Azmi Bin Ismail
Lecturer,
School of Mechanical Engineering
Universiti Sains Malaysia

ii

ACKNOWLEDGEMENT

TABLE OF CONTENTS

LIST OF TABLES

LIST OF FIGURES

LIST OF SYMBOLS

°c   Unit of temperature on the Celsius scale

GREEK LETTER

ε	Epsilon, unit of the permittivity of an insulating
ρ	air density
μ	air dynamic viscosity on the nozzle

LIST OF ABBREVIATIONS

3D	Three-Dimensional
A	Heat transfer area
AL	Acoustic Liner
BAL	Bias Acoustic Liner
CFD	Computational Fluid Dynamics
D_h	Hydraulic diameter of D-chamber (nozzle diameter)
EIDI	Electro Impulse De-icing
ETEDS	Electro-Thermal De-icing System
$\bar{h}$	Convection heat transfer coefficient over entire area
k	Air thermal conductivity
LE	Leading Edge
M	Mach number
m/s	meter per second, SI unit of velocity
MEDS	Mechanical Expulsion De-icing System
mm	Millimeter, SI unit of length in the metric system
Nu	Nusselt Number
Nu_{max}	Maximum Nusselt Number
NTSB	National Transport Safety Board
P	Absolute Pressure
PETDS	Pulse Electro-Thermal De-icing Systems
PIB	Pneumatic Inflatable Boot
PTAI	Piccolo Tube Anti Icing
q	local heat flux density
R	Gas constant, 287
r/D	dimensionless radial distance from centre of plate
Re	Reynolds number
SAI	Swirl anti-icing
$\breve{T}$	Dimensionless temperature
$T\infty$	Ambiance Temperature
$T_{ambient}$	Temperature ambient

Te   Temperature exhaust from hot air-jet

$T_{Exhaust}$ Temperature of the exhaust

TKS   Tecalemit-Kilfrost-Sheepbridge Stokes

T_{nozzle} Temperature of the nozzle

TMEDS   Thermo-Mechanical Expulsion De-icing System

Ts   Temperature surface of the plate

u_0 Outlet velocity of swirling air in D-chamber

LIST OF APPENDICES

ABSTRAK

Sehingga kini, ais di permukaan pesawat dilihat sebagai masalah aerodinamik dan mekanikal yang teruk yang boleh membahayakan keselamatan penerbangan pesawat. Jet udara panas merupakan salah satu kaedah yang digunakan untuk menghilangkan lapisan ais pada permukaan kritikal pada pesawat seperti kulit bibir nacelle. Namun, kesan terus-menerus daripada jet udara panas ke kulit bibir nacelle membentuk titik panas. Oleh itu, projek ini dijalankan dengan kajian berangka pertukaran haba perolakan antara jet udara pada suhu 50 ° C, 55 ° C, dan 60 ° C dan permukaan rata berstruktur menggunakan perisian Fluent untuk mengurangkan titik panas pada permukaan. Standard k-ε model dan tenaga digunakan pada jet model dalam domain tiga dimensi dengan persempadanan ditetapkan. Julat nombor Reynolds yang digunakan dalam simulasi adalah 2000–5000, sementara jarak jet-ke-sasaran mempunyai nilai pemalar pada 37.05 mm menggunakan muncung bulat 2.5 mm. Plat sasaran iaitu plat keluli, tembaga, dan aluminium rata dengan ketebalan 1 mm, 2 mm, dan 3 mm. Kesan aliran dari nombor Reynolds pada sebaran suhu keatas plat rata dapat dilihat bahawa pada 50 ° C ke atas plat keluli 1 mm, nombor Reynolds 4085.86, $\check{T}$ meningkat kepada 0.0734, dan $\check{T}$ menurun kepada 0.0483 apabila nombor Reynolds (Re) 2200.08. Seterusnya, hubungan antara maksimum nombor Reynolds dan maksimum nombor Nusselt terhadap kajian penyebaran udara panas mendapati bahawa pemindahan haba meningkat dengan halaju dan nombor Reynolds berserta dengan nombor Nusselt pada titik panas. Maksimum nombor Nusselt meningkat dari 4.3213 hingga 5.2620 apabila maksimum nombor Reynolds bertambah dari 2200.08 hingga 4085.86 bagi keluli dengan ketebalan 1 mm. Analisis ketebalan dan jenis bahan pada plat menunjukkan bahawa semakin rendah kekonduksian termal bahan dan semakin tebal plat, semakin lama masa yang diperlukan untuk mengalir haba panas untuk melalui plat. Tembaga dengan ketebalan 3 mm pada suhu jet 55 ° c, menunjukkan perubahan yang laju untuk sebaran suhu pada plat permukaan iaitu 0.0391. Sebaliknya, keluli dalam keadaan yang sama menunjukkan perubahan termal yang perlahan terhadap plat permukaan 0.290 pada nombor Reynolds 4085.86. Kesimpulannya, keluli pada ketebalan 3 mm dengan suhu udara panas antara 50°c hingga 60°c berserta kesemua nombor Reynolds adalah model terbaik untuk meminimumkan titik panas atau pemanasan permukaan.

ABSTRACT

Until recently, ice on an aircraft's surface was seen as a severe aerodynamic and flight mechanical problem that may jeopardise aircraft flight safety. Hot air jet impingement is one method used to eliminate icing on critical aircraft surfaces such as the nacelle lip skin. However, due to the direct impact of the hot air jet on the nacelle lip skin, a hotspot was created. Thus, this project is concerned with a numerical study of the convective heat exchange between an impinging air jet at temperatures of 50° C, 55° C, and 60° C and a structured flat surface using the Fluent tool to reduce the hot spot on the surface. Standard k-ε model using the energy equation are carried out on a model jet in a three-dimensional domain with periodic boundary conditions. The range of jet Reynolds numbers utilised in the simulations is 2000–5000, while the jet-to-target distance remains constant at 37.05 mm using a circular 2.5 mm nozzle. The target plate is flat steel, copper, and aluminium plate with a 1 mm, 2 mm, and 3 mm thickness. The effect of Reynolds number impingement flow on temperature distributions on a flat plate can be seen that at 50°C for a 1 mm steel plate, the Reynolds number is raised to 4085.86, the $\breve{T}$ is increased to 0.0734, and the $\breve{T}$ is decreased to 0.0483 when Reynolds number (Re) of 2200.08. The relationship between Reynolds number and Nusselt number to the hot air impingement study was found that heat transfer rises with velocity and Reynolds number and subsequently with Nusselt number on the impinging point. The maximum Nusselt number increases from 4.3213 to 5.2620 when the Reynolds number grows from 2200.08 to 4085.86 for 1 mm thick steel. Material type and thickness on dimensionless temperature were examined. The thickness and material analyses on the flat plate showed that the lower the thermal conductivity of the material and the thicker the plate, the longer it takes for heat to flow through the wall. Copper with a thickness of 3 mm at 55° C air-jet temperature exhibits a fast change in thermal performance on a 0.0391 surface plate. In contrast, steel with identical conditions shows a sluggish change in thermal performance on a 0.290 surface plate at a Reynolds number of 4085.86. In conclusion, steel at a thickness of 3 mm with hot air temperatures ranging from 50° C to 60° C also all Reynolds number is the best model for minimising hot spots or surface overheating.

CHAPTER 1

INTRODUCTION

1.1 Overview of the project

Aircraft icing continues to be a critical aviation hazard as the global fleet of commercial airlines, regional business jets, and general aviation aircraft continues to grow. Most aviation icing accidents occur because of ice accumulation on the aerodynamic surfaces of the aircraft, such as the leading edges of the tail and the nacelle lip-skin surface [1]. Ice accumulation impairs performance and handling characteristics significantly, posing substantial safety concerns [2]. An example of an air accident due to ice accumulation was an Embraer EMB-500 Phenom's aircraft crashed on Dec. 8, 2014, into a neighbourhood at Gaithersburg, Maryland. According to the National Transport Safety Board (NTSB), the crash was caused by an in-flight icing situation where the pilot failed to turn on the anti-ice system. The aircraft had been in icing conditions for about 15 minutes on approach with clouds and snow encountered was approximately 2.8 nautical miles from the destination of Gaithersburg-Montgomery County Airport. As a result, airspeed resumed its downward trend, and the airplane began to roll to the right before starting to roll to the left then crash. Thus, the pilot fails to turn on the airplane's wing and horizontal stabiliser de-ice system, leading to ice accumulation on those surfaces after losing aircraft control [3].

Therefore, ice on aircraft components must be removed and/or avoided, if possible, to ensure the aircraft's performance and operation are not compromised. Even little quantities of ice may wreak damage. Consequently, several techniques have been developed for avoiding and eliminating ice. Anti-icing and de-icing methods are the two fundamental types of ice management procedures. Methods for de-icing are used to remove ice that has collected after and during ice build-up on the outer surface. Ice protection devices that use de-icing methods include a Pneumatic Inflatable Boot and an Electro Magnetic Expulsion. Anti-icing systems are designed to reduce or eliminate ice accumulation on protected surfaces significantly. Thermal and chemical fluids are both commonly employed as anti-icing methods. The two different types of ice protective devices that use thermal anti-icing systems are electric heater anti-icing and hot air anti-icing. Anti-icing devices that use heated bleed air, particularly SAI and

Piccolo Tube Anti-Icing (PTAI). Piccolo Tube Anti Icing (PTAI) has been the major method of preventing ice accumulation on the nacelle lip skin of modern commercial transport aircraft [4].
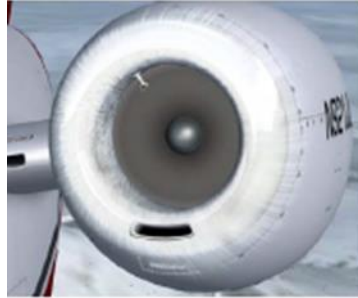
Figure 1.1   Nacelles Lip Skin

As previously stated, the growth of commercial airlines, regional business jets, and general aviation aircraft has been followed by an increase in noise levels. To address this, the Federal Aviation Association has established aircraft noise regulations to which all aircraft manufacturers must conform. There are various methods for lowering engine and turbine noise, for example, installing an acoustic liner (AL) in a noise cowl zone. As nose cowl zones are limited in size, Lucas [5] recommended installing a noise abatement system on the leading edge of the nacelle. However, the combination of an acoustic liner and anti-icing on the leading edge of a nacelle may be unable to efficiently reduce forward radiated noise and increase the thermal performance of the anti-icing system. As a result, a bias acoustic liner (BAL) is placed in that limited area to compensate for the heat transfer to the nacelle lip cowl zone being non-uniform [6] [7].

However, even though PTAI is very effective at avoiding ice build on the aircraft's surface, it results in a significantly non-uniform temperature distribution along the nacelle lip, leading to the formation of a hotspot. In addition, impinging jets of PTAI with a high temperature and velocity that are focused (concentrated to a point on the surface) along the inner skin of the nacelle lip may cause damage or destruction to the nacelle lip-skin material, Acoustic Liner, and Bias Acoustic Liner, since the Acoustic Liner and Bias Acoustic Liner may possibly be positioned on the inner skin of the nacelle lip. As a result, runback icing develops downstream of the nacelle lip, increasing aircraft noise [8].
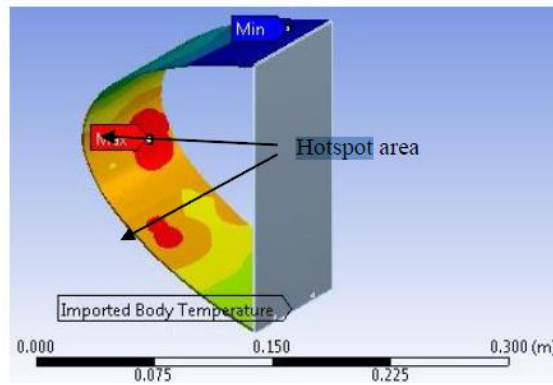
Figure 1.2   Temperature contour of nacelle lip-skin [9]

This project is performed using a single impinging jet on a flat plate to study the effect of impingement hot air on temperature distribution by using a numerical method on the variable controlled of temperatures, velocity, materials, and thicknesses.

1.2   Problem Statement

First, the reasons for ice accumulation on the wing leading edge and nacelle lip-skin vary according to the natural environment and the aircraft's conditions, which may result in fatal aviation accidents as it influences by aerodynamic performance. Therefore, the piccolo tube anti-icing system is installed to prevent ice accumulation. Acoustic Liner and Bias Acoustic Liner are introduced on the nacelle lip skin to enhance an aircraft's noise abatement system. However, the piccolo tube anti-icing system employs a non-uniform distribution of high temperature and velocity from the impinging jet to maintain the inner skin heated and free of ice. It generates hotspots that may cause damage or destruction of nacelle lip-skin material, Acoustic liner, and Bias Acoustic Liner. As a result, runback ice forms downstream of the nacelle lip, contributing to increased aircraft noise.

1.3   Objectives

The objectives of the study are as follows:

1)   To develop a three-dimensional (3D) numerical simulation of hot air impingement flow.

2)   To study the effect of Reynolds number impingement flow on temperature distribution on a flat plate.

3)   To study the relationship between Reynolds number and maximum Nusselt number to the hot air impingement study.

4)   To study the effect of material type and thickness on temperature distribution.

1.4   Outline the Scope of The Project

This study uses Ansys Fluent Software to simulate an impingement hot-air anti-icing system in a three-dimensional (3D) model. The Reynolds number is the parameter that affects this thermal performance while analysing the flow structure and heat transfer.

This study involves compressible fluid flow in a steady condition. The standard k-ε model with standard wall function was carried out in the turbulent model. Air jet flow onto a single circular nozzle flow that impinging on flat plate comprises of three different thicknesses (thickness = 1mm, 2 mm, 3mm) that was conducted by varying the jet velocity of nozzle exit (V=14 m/s,16 m/s,18 m/s,20 m/s,22 m/s,24 m/s,26 m/s), the temperature of hot air (T_e= 50°c, 55°c, 60°c). Aluminium, steel, and copper are added as the materials of the plate with their respective properties. The boundary is chosen based on its name, type, and values for the effect of temperature and velocity applied. When hot air is bled, the temperature and pressure of the air are controlled before it is directed into a container via a nozzle. The jet velocity exiting the nozzle influences the Reynolds number, as does the temperature of the hot air. The simulation is then run using the simple scheme method and standard initialisation to finish the computation. The results will be confirmed by comparing theoretical average Nusselt numbers to the simulation result of average Reynolds and average Nusselt's numbers.

CHAPTER 2

LITERATURE REVIEW

2.1 Ice Protection System

There are several types of ice protection systems which are mechanical, fluid, thermal, and hybrid. Generally, operation principles for fluid ice protection systems are by lowering the freezing point below the ambient air temperature where it mixed with impinged water. In contrast, Mechanical ice protection systems will destroy the bond of ice from the aircraft surface, then the pieces of broken ice were blown away to atmospherics. A thermal ice protection system using hot air or electric power as a heat source provides heat to the protected aircraft surface. Finally, a hybrid ice protection system consists of a running wet electro-thermal anti-icing system and an EMEDS. The electro-thermal running wet system keeps sensitive zones above freezing temperature, and the actuators of the EMED system periodically remove ice that accumulates the result of runback freezes downstream.

2.1.1 De-icing

A mechanical de-icing device such as Electro Impulse De-icing (EIDI) is based on electromagnetic forces to remove ice from a surface. Albert C. Kodet states that these systems use resistance pads, heat the airfoil above melting ice temperature, and thus allow the accumulated ice to be moved by the air stream requires large amounts of electrical and energy. This limits their application to small surfaces such as engine inlets [10]. Other than that, a pneumatic inflatable boot (PIB) has an inflated rubber boot on the wings and control surfaces to which the de-ice is attached. After building up a controlled ice layer, compressed air inflates the de-ice. The inflating cycle takes a few seconds to achieve optimum ice shed and prevent further ice development on the inflated surface. Then de-ice may deflate by draining air into the atmosphere [11].
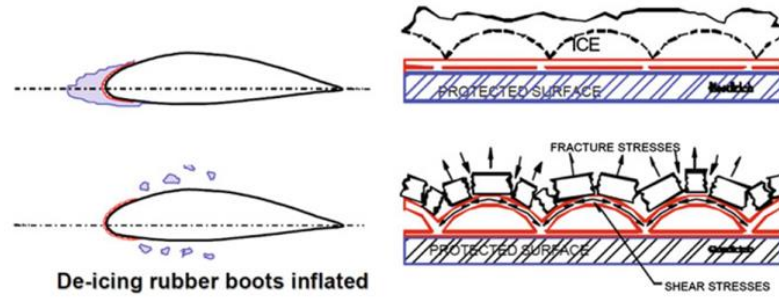
Figure 2.1   Working principle of Pneumatic Inflatable Boot (PIB) [11].

Goodrich's state thermal ice protection Pulse Electro-Thermal De-icing Systems (PETDS) uses an electro-thermal pulse approach. PETDS contain strips and shedding zones as heating components. The partition strips maintain surface temperature above freezing while shedding zones melt the ice contact on the leading-edge surface. While for Flying Crane, Electro-Thermal De-icing System (ETDS) is constructed. However, the same operating concept as PETDS, runback water refreeze is challenging to manage, and ice formation may occur outside the ice protection area. Therefore, aircraft with ETDS should rapidly escape from icing encounters when significant icing severity occurs [12].

Thermo-Mechanical Expulsion De-icing System (TMEDS), a hybrid system, was designed to provide ice protection on icing surfaces at even lower power to achieve roughness-sensitive air foils. TMEDS use a resistive heater connected to the area of the leading edge to be protected, with particular attention on the impingement zone where the incoming air stream divides between the upper and lower surfaces. However, TMEDS undoubtedly demands a high cost, and the criteria for engineering applications require additional time. Thus, lengthy flight time in icing circumstances may compensate for TMEDS [13].

2.1.2 Anti-icing

The most typical thermal anti-icing systems used for nacelle and wing ice protection run in two modes: evaporative or running wet. The surface is heated sufficiently to prevent runback beyond the heated zone during an evaporative technique. In contrast, the surface is heated to avoid freezing within the heat zone during the wet running technique. In the hot air system, the hot air heat is transferred to the lip-skin nacelle. This energy is required to evaporate impinging water and maintain the lip-

6

temperature skin above freezing. The engine compressors deliver high-temperature and high-pressure hot air heated via a conduit/supply pipe known as a piccolo/perforated tub. Then goes around the D-chamber [14].
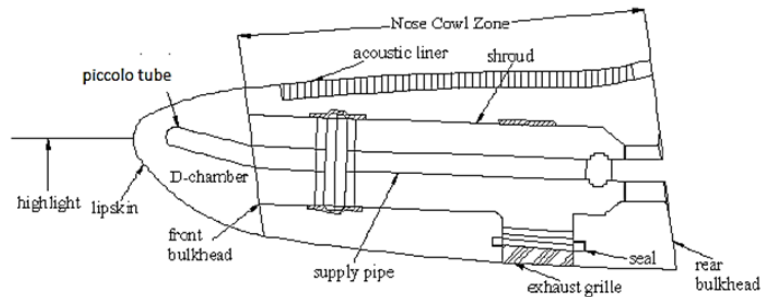
Figure 2.2   Part of nacelle intake [14].

Electro-thermal ice protection systems may also be utilised in anti-icing mode that may be installed in a critical area such as nacelle lips, windshields, and parameters compared to de-icing. Unlike icing, this mode activates partition strips sequentially for power conservation. Electro-thermal anti-icing uses too much energy that requires electricity. Therefore, de-icing on broad surfaces is more practicable [12].

A hybrid anti-icing system applies a similar concept to TMEDS, this system consisting of an electro-thermal heater (EIDI or EMEDS) followed by a Low Power De-icing System. However, unlike methods using the "parting strip" concept, the current LPDI does not require the leading edge (LE) thermal system to function. Instead, it indicates some frozen runback that extended beyond the protected zone of the de-ice. This was a warm and high liquid water content condition [15].

TKS Ice Protection is chemical ice protection that dispenses an ethylene glycol-based fluid by lowering the freezing point through laser-drilled titanium panels on the leading edges of the wings, horizontal and vertical stabilisers, and a slinger ring protects the propeller. As air flows over the wing and empennage, it disperses the fluid, coating the surfaces and preventing the formation and adherence of iced [16].

2.2   Fluid Flow Theory

2.2.1   Heat convection (Heat transfer for impingement jet)

Simionescua, Corneliu Bălana highlighted those three zones that are often used to classify impinging jet flows: First, the free jet region is defined as the zone within which the impingement plate does not affect the flow. The velocity is predominantly axial and consistent along the jet centerline in this zone. Second, the flow is diverted away from its axial direction toward a radial direction in the stagnation area. Thirdly, the velocity in the wall jet zone is mostly radial, with the formation of a boundary layer along the radial direction. The boundary layer velocity profile is formed similarly to a wall jet, with the highest velocity occurring at a point intermediate to the wall. Its thickness grows as the radial distance rises, but its maximum velocity decreases [17]
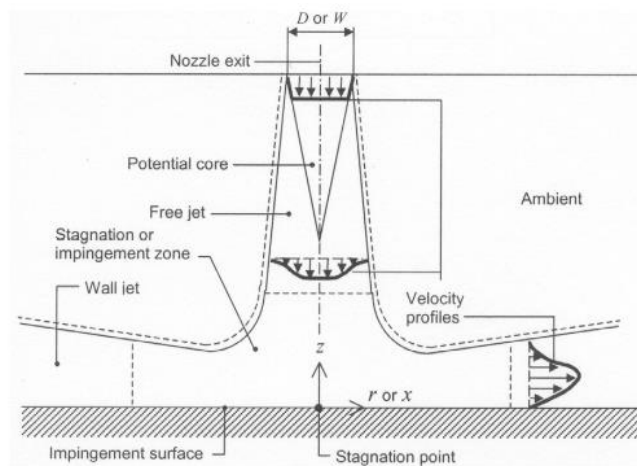
Figure 2.3   The flow regions of an impinging jet [17]

In this case, the air jet emerges perpendicular to the impingement plate from the circular nozzle. Air jet impingement is a kind of forced convection heat transfer. Forced convection is a heat transfer process in which fluid motion is created externally. This type of heat transfer is used in various standard devices, including air conditioning, central heating, and other different processes. The Reynolds number and the distance between the jet exit and the wall are critical parameters[17]. Given that the parameter under consideration is the Reynolds number by the project aims to optimise it, the jet's exit and other parameters were ignored.

2.2.2   Reynolds Numbers

Reynolds number (Re) is a dimensionless number used in fluid mechanics to denote the ratio of inertial to viscous forces. On the other hand, Reynolds was the first to establish criteria for identifying laminar from turbulent flows. In this research, a fully turbulent flow was considered to be the condition for the flow of a circular nozzle. According to Frank P. Incropera et al., when (r/D)>10, the turbulent flow from a rounded converging nozzle should be fully developed.[18].

Limaye et al. investigated the effect of Mach number and Reynolds number on the heat transfer distribution in the presence of a flat-plate impingement jet. Investigators discovered that increasing the Reynolds number enhanced the heat transfer rate at all radial distances from the stagnation point specified by Saulo A. G. Salcedo et al.[19].

2.2.3   Heat conduction (Heat transfer for plate condition)

According to Fourier's law of heat conduction that Mohd Azmi [8] analysed, it's has shown that any given air thermal conductivity, the heat transfer from the surface to the fluid is significantly dependent on the temperature gradients within the boundary layer. Because of the thinner boundary layer of impingement, there is a more significant temperature gradient, which increases the rate of heat flux from the surface. The boundary layer thickness decreases as the velocity of the external flow rises, increasing the temperature gradient. Consequently, the heat transfer coefficient increase

$$q = -k\Delta T \qquad\qquad 2.1$$

Where,   q = heat flux
              k = thermal conductivity
              $\Delta T = T_{hotair} - T_{surface}$

According to Newell Thomas's analysis of heat flux, the area, temperature differential, and thermal conductivity all rise proportionately as the heat transfer convection increases. Conversely, as the thickness increases, the heat transfer convection reduces [20].

$$Q = -\frac{Ak}{t}\Delta T \qquad\qquad 2.2$$

Where,   Q = Heat transfer conduction
      A = area
      t = thickness
      T_{sur} = Surface temperature
      T_{amb} = Ambient temperature

2.2.4 Relationship between Reynolds Number and Nusselt Number

M. Molana and S. Banooni found that when a single free liquid jet was used to study heat transfer, the local and Nusselt numbers were higher than in the streaming flow zone, based on numerical or experimental findings. This is because the area's fluid film thickness is considerably thinner than in the surrounding region. This implies a higher mean fluid velocity in this region. Additionally, a significant degree of agreement has been found between the computational and experimental results for single jets. Local and Nusselt populations rise as the number of Reynolds increases [21].

A significant agreement is seen in Abdulrahman Alenezi's work, which discusses the study of heat transfer distribution on a uniformly heated flat plate caused by circular air jet impingement. Their study focuses on local and average Nusselt numbers for low Reynolds number flows and small jet-plate distance. In their experiments, H/D ratios of 1 to 12 were tested at a typical radial distance from stagnation point, 0-10 r/D. Nu has a clearly defined stagnation point peak for all Re values [22].

2.2.5 Type fluid Flow conditions

Incompressibility is a precondition for this project. This condition describes a flow with constant densities. In this study, when gas molecules are forced through tube walls, they are deflected by the tube walls. When a gas moves at a rate considerably slower than the speed of sound, its density remains constant as the flow velocity rises. However, when the flow velocity approaches the speed of sound, it is reasonable to examine the gas's compressibility [23]. The gas's density fluctuates depending on its location. Nevertheless, the gas density remains constant because the Mach number does not approach one. The calculation of Mach number shows the necessity to identify fluid

regimes with incompressibility effects. The ratio of the sound speed in air to the speed of sound determines the number of different compressibility effects [24][25].

$$M = \frac{v}{c} \qquad\qquad 2.3$$

Where   v = local velocity, m/s
             c = speed of sound, m/s

The speed of sound in metric units is computed as [26]

$$c = 20.05 \, (273.16 + t)^{\frac{1}{2}} \qquad\qquad 2.4$$

Where   c = velocity of sound (m/s)
                       t = temperature ($^\circ$ C)

The incompressible condition is shown below.

Condition: velocity of air jet 14 m/s at 50^0 C

$$c = 20.05 \, (273.16 + 50)^{\frac{1}{2}} = 360.432$$

The Mach number = 0.039 <1

2.3   Computational fluid dynamic (CFD)

K. Lakshmi Prasad, who used computational fluid dynamics to study hot-turbulent crossflow jet flow (CFD). The standard k-ε turbulence model is used, and the three-dimensional flow field is estimated [27].

Shashikant Pawar and Devendra Kumar Patel noted the studied of the flow dynamics under normal impingement of twinjets that using two-equation turbulence models. For both partly recirculated and nonrecirculating twin jets, simulations were performed using standard k-ε, realisable k-ε, and standard k-ε models. The findings indicate that the standard k-ε model is unable of accurately predicting twin-jet, while the standard k-ε and realisable k-ε models exhibit the greatest agreement with the experimental data [28].

Wang and Mujumdar's investigation on limited turbulent slot jet models. They revealed that models could predict the overall shape of the Nu number distribution but overestimate the stagnation point and prove that models perform better at the high jet to plate distances in the stagnation zone [29].

According to Baughn and Shimizu, Lytle and Webb, and Elison and Webb, the number of jets, jet to target distance, and turbulence intensity are critical operational variables that affect the amount of heat transfer coefficient as highlighted by P. Chandramohan et al. [30].

Merci and Dick investigated heat transfer for turbulent axisymmetric jets impinging on a flat plate using the cubic k-model. Their results indicated that the Nusselt number decreases from the stagnation point's peak value to a minimum value, then increases to a maximum value and decreases again as the downstream distance increases [31].

CHAPTER 3

METHODOLOGY

3.1   Introduction

This chapter discusses the methods and processes used to accomplish the research's goals. The chapter is divided into two sections: the general overview and the flow fluency methods.

The goals of this research are to, first, to develop a three-dimensional (3D) numerical simulation of hot air impingement flow; second, to study the effect of Reynolds number impingement flow on temperature distribution on a flat plate; third, to study the relationship between Reynolds number and maximum Nusselt number to the hot air impingement study; and fourth, to study the effect of material type and thickness on temperature distribution.

3.2   The Overall Views

The study was conducted using a quantitative methodology. The methodology process entails defining the problem, designing it precisely, and analysing it. This endeavour will take roughly two semesters to complete. After that, the documentation and writing of the thesis were completed. The methodology's flowchart is shown in Figure 3.1.
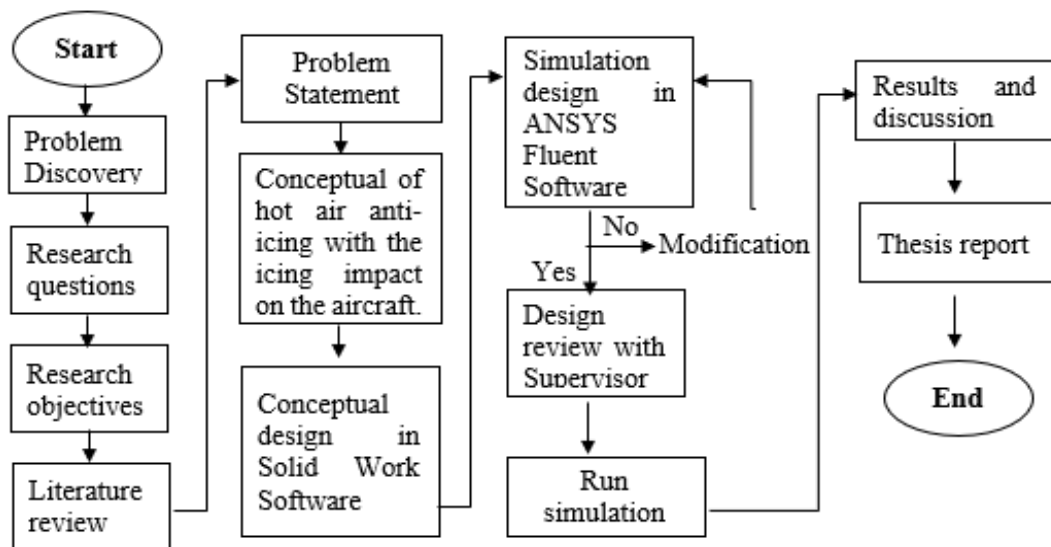
Figure 3.1   Flow chart of overall work

The initial phase of implementing this project begins with problem discovery. Ice accretion on the critical surface is the implication of hotspot tube in nacelle lip skin by operations of piccolo tube during surface area exposed to cold air flows free streams toward to aircraft. Ice accretion may cause damages to the engine and noise abatement devices or even destroy the engine compressor blade. In addition, the combustion chamber as the ice may shed and be ingested into the engine or hit the blades. It is occurring during temperature is above freezing point, visible moisture, or high humidity.

The most important part of the research project is the research question. All the questions should be focused, specific, appropriately complex, and relevant to the issue. For example, why the simulation of temperature profiles of hot air impingement is needed in this research project? And what is the correlation between Reynolds number and maximum Nusselt Number? These two questions are defined as the concepts of the research question more clearly.

The collecting data and research questions that summarise the findings and provide direction for further analysis of the study area must be feasible to establish a research project's appropriate scope and objectives. This project aims to, first, to develop a three-dimensional (3D) numerical simulation of hot air impingement flow; second, to study the effect of Reynolds number impingement flow on temperature distribution on a flat plate; third, to study the relationship between Reynolds number and maximum Nusselt number to the hot air impingement study; and fourth, to study the effect of material type and thickness on dimensionless temperature.

After that, a review of the existing literature will be conducted. It is to understand and familiar with the current research and concerns in the topic of study. In this thesis, there is the following knowledge that studied: the theory of anti-icing system and a de-icing system, the hot air jet impingement, type fluid flow, Reynolds Number, Nusselt Number, and the effect based on method parameter study. Next is the problem statement. It is briefly explaining the problem of the research project. The problem in this project is more focused on the implication of hotspot hot air jet impingement during impinging jet, which is ice accretion and damage of noise abatements devices.

The concept of hot air anti-icing with the icing impact on the aircraft is developed. Next, the 3D impingement jet on the flat plate is designed and edited on

SolidWorks software until the supervisor approves the design. The simulation is then run, and the results are retrieved using the Ansys Fluent programmed. Finally, the thesis report is written to justify the completion of an academic degree.

3.3   Computational Setup

Based on Figure 3.5, software was utilised to simulate the parameters of the hot air impingement in the domain. A three-dimensional hot air impingement was designed in SolidWorks software using hot air anti-icing characteristics, as shown in Figure 3.2 and Figure 3.3. The design was divided into 19 smaller volumes of bodies discretised independently to facilitate meshing and get the desired structured mesh. The file is then exported to design modelers in a file. STEP output format (ANSYS Workbench-compatible format) for usage with ANSYS Software. The STEP file in which the geometry information is exported in a standard format for usage across several Cad software prevents file exportation errors. The geometry may be adjusted after exports, which is helpful for the design process. [32]
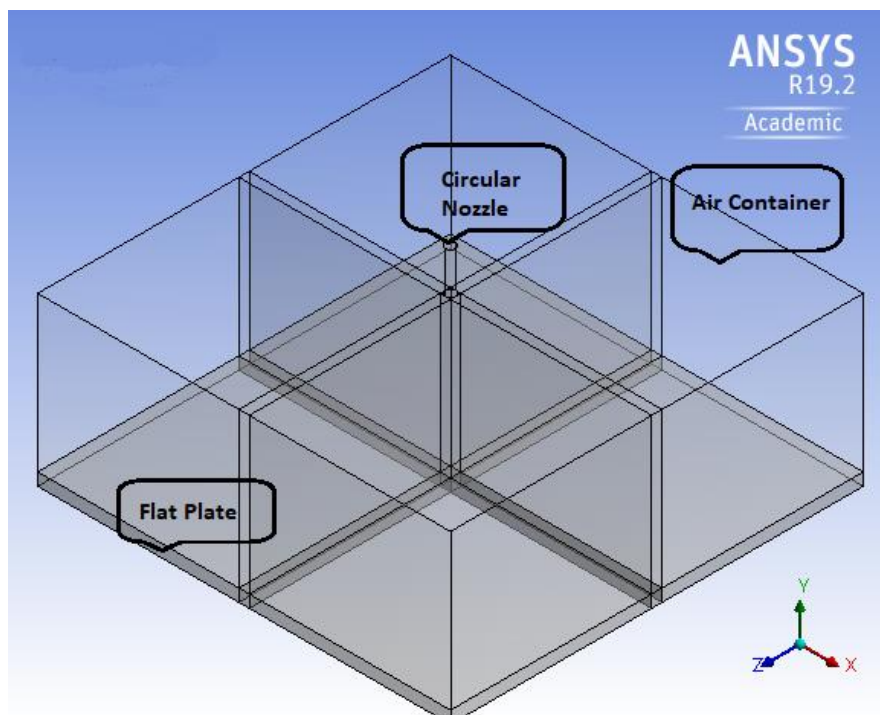
Figure 3.2   Isometric View of jet impinges to flat plate system
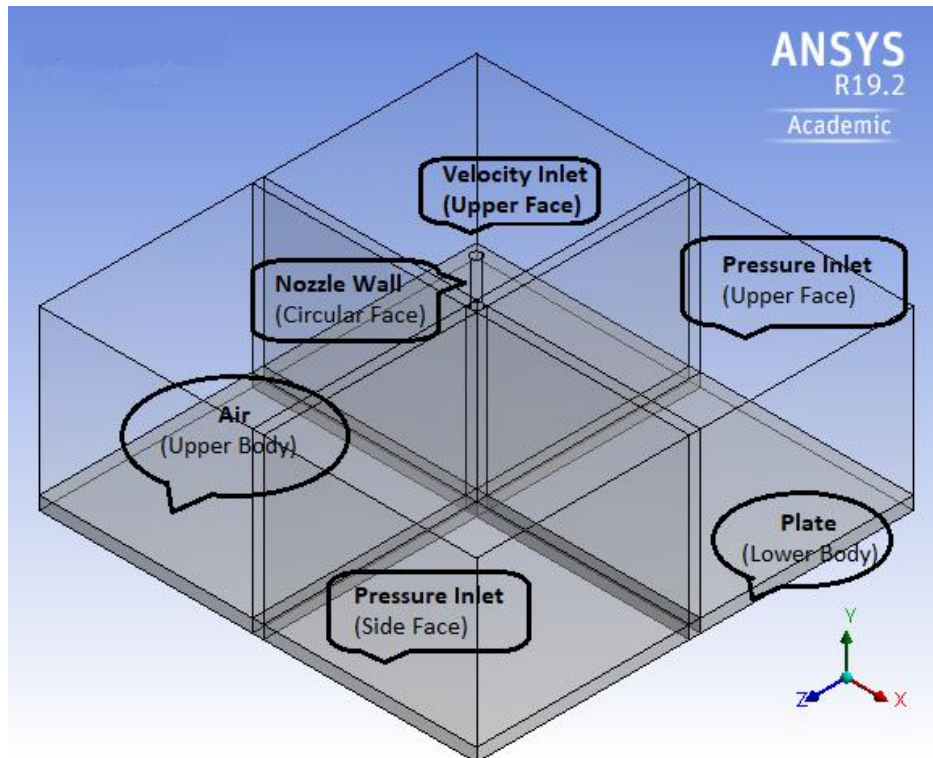
Figure 3.3   Boundary conditions of jet impinges to flat plate

Boundary Meshes for three-dimensional surfaces have constructed the air container and plate using the edge sizing method to avoid excessive mesh elements and lengthy computation time. The grid is refined along the stagnation zone and wall jet regions to identify temperature changes with a bias factor of 20 in these regions. The Automatic Method, Multizone, and Face Meshing were used to enhance the mesh of circular shapes on the nozzle body. The mesh improvements are applied during the setup process until the mesh is complete. Then, the geometry at each area of bodies is subjected to boundary conditions, including plate, air, pressure outlet, pressure inlet, nozzle wall, and velocity inlet.

Before analysing the dimensionless temperature profiles on the flat plate surface, a grid independence test was conducted to ensure that the simulation results are accurate at the optimal mesh size. Table 3.1 and Figure 3.4 compares the sensitivity of three different meshes to the temperature profiles. As demonstrated in these data, the outcomes for fine and very fine meshes are comparable. For comparison purposes, consider a fine mesh of 358726 grid elements that converges in about two hours. On the other hand, very fine meshes contain 1881200 grid components and take four hours to

converge in a single instance. As a result, the current mesh was selected for all computational models in the research to reduce computing time.

Table 3.1   Grid parameters used for mesh sensitivity

Grid	Element	Temperature (°c)
Course	8617	29.48
Fine	358726	27.96
Very Fine	1881200	27.20
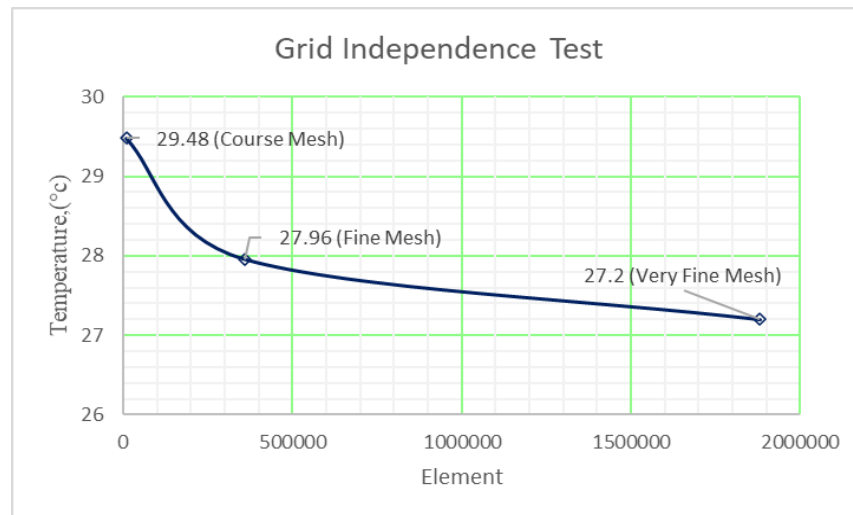
Figure 3.4   Grid Independence Test.
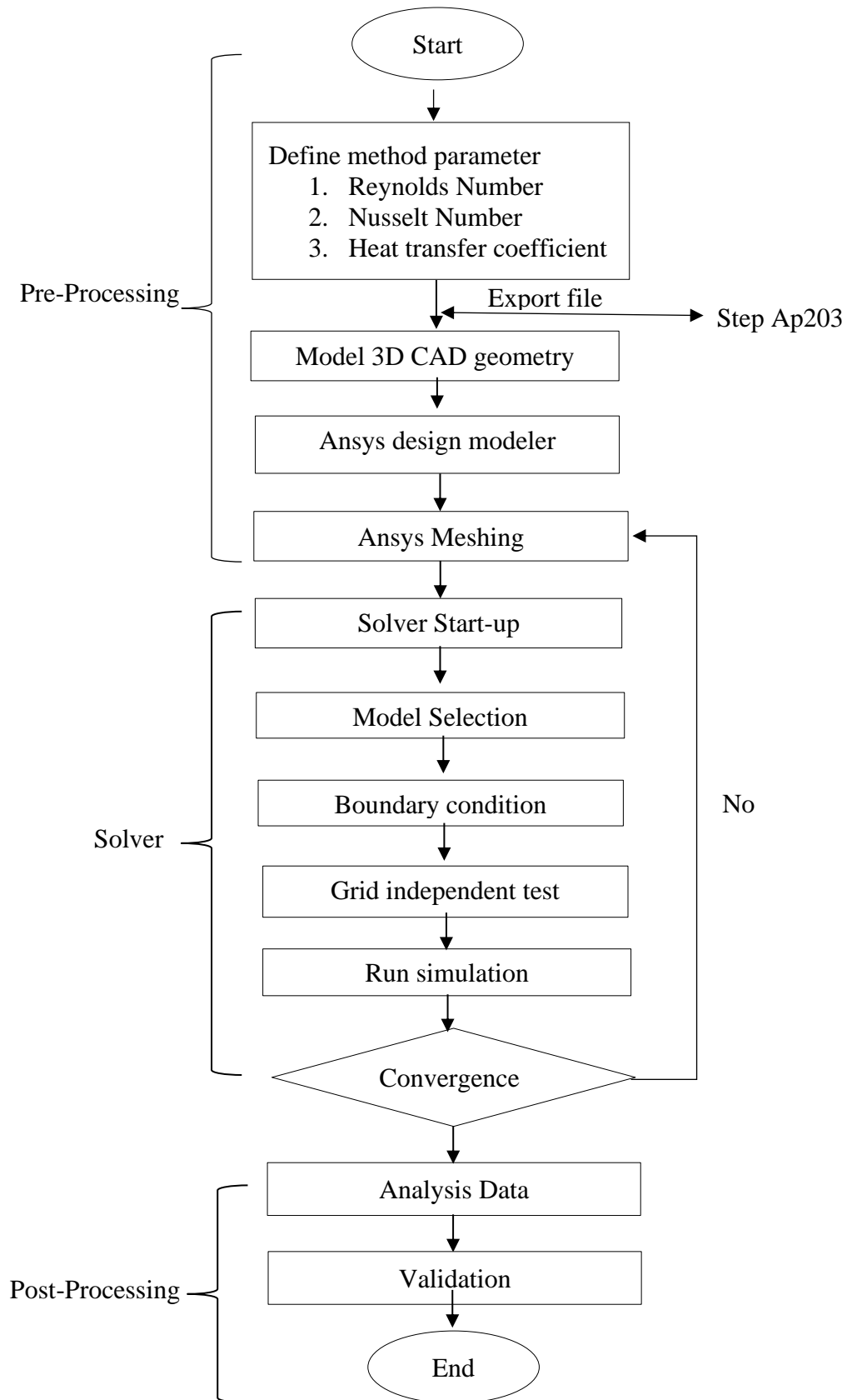
Figure 3.5   Flow Fluent chart

The next step is to start the solver. When the Setup feature is enabled, the Fluent Launcher window appears. The Processing Option is specified to Series (Local Machine). A steady-state model of flow and heat transfer was developed. The energy model has been activated because simulations involving heat transfer necessitate the use of an energy model. The selection of models is then carried out. Standard k-ε are used to simulate incompressible flows. A standard wall function with near-wall treatment is used to capture turbulent flow characteristics in this research project.

Aluminium, Steel, and Copper are applied to the plate (solid type) as materials with the properties listed in Table 3.2. Following the material selection, the computational boundary conditions for each material are listed in Table 3.3, along with their types and values for the effect of applied velocity and temperature. The pressure field was evaluated using the pressure-velocity coupling method (SIMPLE) (Semi Implicit Method for Pressure-Linked Equations). The turbulent kinetic energy and turbulent dissipation rate equations are solved using a first-order upwind discretisation scheme. The momentum, energy, and density equations are solved using a second-order upwind discretisation scheme. When the energy equations reach a value of 10^{-3}, the solutions are converged. Once the energy does not converge, the solution under the relaxation factor is modified by increasing or decreasing the pressure or energy value until the convergence parameter variables are acceptable.

Table 3.2   ANSYS Material Properties Library of Aluminium, Copper and Steel

Property	Aluminium	Copper	Steel
Density (kg/m^3)	2719	8978	8030
Specific Heat (J/kg. K)	871	381	502.48
Thermal conductivity (W/m. K)	202.4	387.6	16.27

Table 3.3   The selection of boundary according to their conditions and values for hot air impingement on flat plate

Boundary Conditions	Position	Value
Pressure Outlet	Side face of air container	Temperature: 27°c
Pressure Inlet	Upper face of air container	Temperature: 27°c
Velocity Inlet	Upper face of nozzle	Velocity magnitude: 14 m/s,16 m/s,18 m/s, 20 m/s ,22 m/s ,24 m/s ,26 m/s Temperature: 50°c, 55°c, 60°c

The simulation is then run with standard initialisation, which computes from the velocity inlet to the end of the calculation. The simulation takes approximately 1 to 2 hours to complete because the number of iterations used is between 1000 to 3000. Results were analysed in the post-processing setup.

3.4   Data Reduction

3.4.1   Reynolds Number

Reynolds number (Re) is an important parameter as it can be used to differentiate layers in flowing fluid between laminar and turbulent flows [33]. The following equation is used to calculate the Reynolds number:

$$Re = \frac{\rho u_o D_h}{\mu} \qquad 3.1$$

where: ρ = air density
μ = air dynamic viscosity on nozzle
u_o = outlet velocity of swirling air in D-chamber
D_h = hydraulic diameter of D-chamber (nozzle diameter)

The density of air, ρ is based on change with respect to the temperature related to the effect of exhaust area on the PTAI thermal performance. Airflow was incompressible and turbulent. It was assumed that air characteristics followed from an equation of state (Ideal gas law) relating density and temperature

$$P = \rho RT \qquad 3.2$$

where   P   = absolute pressure
ρ = air density
R   = gas constant
T   = air temperature

Rearrange the equation, average air density, ρ is determined by:

$$\rho = \frac{P}{RT} \qquad 3.3$$

3.4.2   Nusselt number

The Nusselt number on the impingement surface is calculated to investigate the influence of impingement ranges on the Reynolds number. The Nusselt number must be determined because it was directly proportional to the Reynolds number as a function of the hydraulic diameter parameters. The equation for the Nusselt number is as follows: [8]

$$Nu = \frac{\bar{h}D_h}{k}$$
<div align="right">3.4</div>

where $\bar{h}$ = convection heat transfer coefficient
                        over entire area
               D_h = hydraulic diameter of D-chamber (nozzle
                        diameter)
               k   = air thermal conductivity

The convection heat transfer coefficient over the entire area, $\bar{h}$ can be obtained from an equation of heat convection.[8]

$$Q_{convection} = \bar{h}A\left(T_{hotair} - T_{surface}\right)$$
<div align="right">3.5</div>

where $\bar{h}$ = convection heat transfer coefficient   over
                        the entire area, W/m^{2}K
               A = heat transfer area, m^2
            T_{hotair} = temperature of the hot air from the nozzle, K
            $T_{surface}$ = temperature of the surface, K

Rearrange the equation, convection heat transfer coefficient over the entire area, $\bar{h}$ is determined by:

$$\bar{h} = \frac{Q_{convection}[W]}{A\,[m^2]\left(T_{hotair} - T_{surface}\right)[K]}$$
<div align="right">3.6</div>

3.5 Validation Result

The findings of numerical simulations were compared to those acquired experimentally. The method for obtaining the numerical solution of an impingement jet on a surface was verified by impinging a single circular jet on a flat plate surface. The average Nusselt number test was used to compare the current study's findings to the experimental results. Wen and Jang recently provided a numerical equation for this benchmark configuration [34].

$$Nu_{avg} = 0.442\, Re^{0.696} Pr^{\frac{1}{3}} (\frac{H}{D})^{-0.20} (\frac{r}{D})^{-0.41}$$

3.7

Range of validity: H/D from 3 to 16, r/D from 0 to 7.14, Re from 750 to 27,000

The validation result is shown in Figure 3.6 with a steel thickness of 1 millimetre and an air jet temperature of 60°c. This section investigates the heat transfer distributions caused by a hot air jet striking a cooled plate at average Reynolds numbers of 2200.07 and 4085.86. These results indicate that the numerical solution has produced the expected physical characteristics of the jet impact with the solid wall.
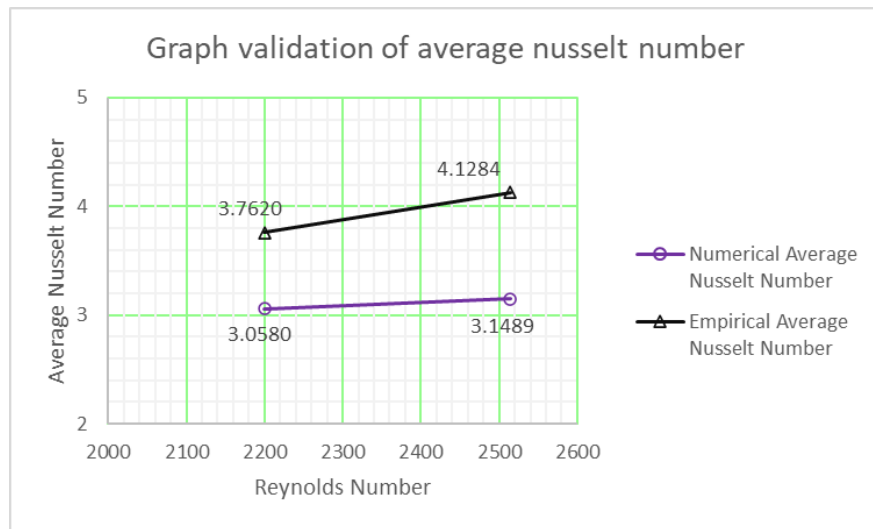
Figure 3.6   Validation Result at a 1-millimetre thickness of the Steel plate

Table 3.4 shows the average Nusselt number result obtained from the numerical results shows good agreement with the experimental and numerical results for a single circular jet compared to the current study of the hot air jet. This validates the model and solution method selected for the current geometry. The numerical results remain within

27% of the average percentage difference for the experimental results validating the numerical procedure. The findings of the percentage difference caused to the total heat input for the experiment are considered equivalent to the total heat loss produced by conduction. The overall heat loss is a function of the temperature differential between the surface and the surrounding environment [35]. In contrast, the heat losses have been ignored in this simulation model to allow for greater accuracy in convective heat flow measurements [22].

Table 3.4   Average Nusselt number result for comparison of experimental and numerical

Reynolds Number	Current Numerical average Nusselt Result	Numerical average Nusselt Result	Percentage Difference %
2200.07	3.058033393	3.761983028	23%
2514.38	3.148883915	4.128375832	31%

CHAPTER 4
RESULTS AND DISCUSSION

4.1   Introduction

This chapter describes and discusses the results from analysing and interpreting the data collected during the research project. The different findings were shown in figures, along with accompanying explanations and discussions. Additionally, it addressed issues raised in the research objective.

4.1.1   The effect of Reynolds number impingement flow on temperature distribution on a flat plate.

Simulation results for the effect of Reynolds number impingement flow on dimensionless temperature ($\breve{T}$) on a plate are shown in Figure 4.1. The dimensionless temperature is present a ratio of the form:

$$\breve{T} = \frac{T_{surfaceplate} - T_{ambient}}{T_{hotairjet} - T_{ambient}} \qquad 4.1$$

The variations of Reynolds numbers of 2200.08, 2514.38, 2828.67, 3142,97, 3457.27, 3771.56 and 4085.86 were applied. The single circular nozzle impinges the hot airflow at three different jet temperatures of 50°c, 55°c, and 60°c with a fixed material made of steel material and 1 millimetre of plate thickness. Figure 4.1 shows the surface temperature plot of the impingement surface for Re = 4085.86 at 55°c of jet temperature to 1 millimetre of steel material.

24